This document is the accepted manuscript version of the following article:
C. Wäckerlin, F. Donati, A. Singha, R. Baltic, S. Decurtins, S.-X. Liu, S. Rusponi, J. Dreiser
Excited Spin-State Trapping in Spin Crossover Complexes on Ferroelectric Substrates
The Journal of Physical Chemistry C, 2018, 122, 8202–8208, https://dx.doi.org/10.1021/acs.jpcc.7b10941

Excited spin-state trapping in spin crossover complexes on ferroelectric substrates

Christian Wäckerlin[†,‡,], Fabio Donati[§,†,¥], Aparajita Singha[†], Romana Baltic[†], Silvio Decurtins[⊥], Shi-Xia Liu[⊥], Stefano Rusponi[†], Jan Dreiser[∥,*]*

[†]Institute of Physics, Ecole Polytechnique Fédérale de Lausanne, Station 3, 1015 Lausanne, Switzerland

[‡]Nanoscale Materials Science, Empa, Swiss Federal Laboratories for Materials Science and Technology, 8600 Dübendorf, Switzerland

[§] Center for Quantum Nanoscience, Institute for Basic Science (IBS), Seoul 03760, Republic of Korea

[¥] Department of Physics - IBS Center for Quantum Nanoscience, Ewha Womans University, Seoul, Republic of Korea

[⊥]Department of Chemistry and Biochemistry, University of Bern, Freiestrasse 3, 3012 Bern, Switzerland

[∥]Swiss Light Source, Paul Scherrer Institut, 5232 Villigen PSI, Switzerland

KEYWORDS

spin crossover, ferroelectric, X-ray absorption, soft X-ray induced excited spin-state trapping

ABSTRACT

We have studied thin films of Fe(II) spin crossover complexes deposited on differently poled ferroelectric PMN-PT $[Pb(Mg_{1/3}Nb_{2/3})O_3]_{1-x}[PbTiO_3]_x$, $x = 0.32$) substrates by X-ray absorption spectroscopy (XAS). The X-ray spectra reveal complete temperature driven conversion between high-spin and low-spin states without any observable effect of the ferroelectric polarization on the spin state of the molecules down to 100 K. In the soft X-ray induced excited spin-state trapping (SOXIESST) regime at 3 K large differences occur between the two ferroelectric polarizations. The efficiency of the X-rays in promoting the molecules to the high-spin state is more than an order of magnitude larger when the ferroelectric dipoles of the substrate are pointing towards the surface as compared to the opposite polarization. We explain our findings by a modulation of the polarization-dependent efficiency of the scattering of X-ray generated secondary electrons at the molecules. Our results provide deep insight into the SOXIESST mechanism and they suggest that such molecules could be used as detectors for electrons traveling in the substrate at energies lower than the substrate electron affinity.

Introduction

Transition metal complexes exhibiting thermal spin crossover (SCO) are interesting for fundamental investigations as well as for applications as molecular switches. Thin films of SCO complexes show potential for molecular electronics and spintronics applications, in particular if their crossover can be controlled by external stimuli such as irradiation by light, interaction with charge carriers or applied electric fields.[1–3] In SCO complexes, the lowest two electronic states having different spin multiplicity are close in energy. In case of Fe(II) SCO complexes the transition occurs between the high-spin $S = 2$ $^5T_2$ state observed at elevated temperature and the

low-spin $S = 0$ $^1A_1$state (O_h notation) at low temperature. The transition temperature $T_{1/2}$ is defined as the temperature at which the high-spin (HS) and low-spin (LS) states are equally populated.[4] The fact that complexes in the LS state can be promoted to the HS state by irradiation with light (light-induced excited spin-state trapping, LIESST)[5–8] allows for an additional degree of control. If the temperature T is low enough, the HS state becomes metastable. In consequence, below T_{LIESST} the HS state can be observed on exceedingly long time scales. Apart from light, other types of excitation can also result in excited spin-state trapping (ESST). Indeed, ESST has been observed as a consequence of nuclear decay (nuclear decay-induced ESST)[4,9], by excitation with "hot" electrons (electron-induced ESST)[10,11], and by irradiation with ionizing electromagnetic radiation such as soft X-rays (soft X-ray induced ESST, SOXIESST)[12,13], hard X-rays (hard X-ray induced ESST)[14] and vacuum-ultraviolet light (vacuum-ultraviolet-induced ESST).[15]

Here, we employ X-ray absorption spectroscopy (XAS) at the Fe $L_{2,3}$ edges, which is well suited to determine the electronic ground state of the Fe(II) ion,[16] to study the thermal SCO and the SOXIESST in thin films of SCO molecules on differently polarized ferroelectric substrates. The SCO complex used in this study is $[Fe(H_2B(pz)_2)_2(bipy)]$ (bipy=2,2'-bipyridine, $H_2B(pz)_2$=dihydrobis(1-pyrazolyl)borate, *cf.* scheme in Figure 1a) which is well characterized in the bulk phase.[17] Furthermore, this compound can be deposited intact by thermal evaporation.[10,18] As substrate, the ferroelectric PMN-PT $[Pb(Mg_{1/3}Nb_{2/3})O_3]_{1-x}$ $[PbTiO_3]_x$, x = 0.32) (011) surface is used.[19,20] The ferroelectric can be poled by application of a strong electric field. In consequence it exhibits a net static electric dipole moment pointing toward the surface ((+)-PMN-PT) or toward the back contact ((-)-PMN-PT). A number of studies report differences in molecular adsorption/desorption[21–23] and selective suppression of thermal SCO depending on

the ferroelectric polarization.[24] However, to the best of our knowledge no effect of the ferroelectric polarization onto SOXIESST has been reported.

Experimental Methods and Materials

Synthesis: $[Fe(H_2B(pz)_2)_2(bipy)]$ has been prepared according to literature procedures.[17]

Sample preparation: The (011) oriented PMN-PT $[Pb(Mg_{1/3}Nb_{2/3})O_3]_{1-x}$ $[PbTiO_3]_x$, x=0.32) substrates (0.5 mm thickness, Atom Optics Co., LTD., Shanghai, China) were cleaned in acetone and isopropanol. Prior to the deposition of the molecules, the substrates were poled in high vacuum by applying $\pm 330\ V$ between two copper electrodes in direct contact with the front and back surfaces of the chip. The $I(V)$ was recorded, and the displacement current caused by the switching of the ferroelectric polarization was observed in order to ascertain that the poling process was successful. In case of a negative applied voltage at the back side of the sample, here referred to as "(-)-PMN-PT", the electric dipole moment points towards the surface. For a positive applied voltage at the back side of the sample, referred to as "(+)-PMN-PT", the electric dipole moment points towards the back contact.

The two thin films of the SCO complex were grown by sublimation of the $[Fe(H_2B(pz)_2)_2(bipy)]$ complexes from a Knudsen cell onto the (+) and (-)-poled substrates concurrently in high vacuum while keeping the substrates at ~10 K in order to obtain a high sticking coefficient of the molecules. The thickness of the obtained films was determined by measuring the step height of an edge produced by masking one part of the sample. The average thicknesses of the molecular films were 75 ± 10 and 65 ± 10 nm on (+) and (-) polarized PMN-PT, respectively. Between the poling process, the deposition of molecules and the XAS experiments, the samples were exposed to air. The powder sample was produced by pressing the polycrystalline powder of molecules on an indium foil.

X-ray absorption spectroscopy: The XAS experiments were performed at the X-Treme beamline[25] (Swiss Light Source, Paul Scherrer Institut) in total electron yield (TEY) mode. The beam was defocused (0.3 x 1.2 mm^2) and spectra were normalized to the TEY measured simultaneously on a gold mesh. The photon flux was measured at the same fixed energy on the gold mesh which was referenced to a calibrated photodiode after the last optical element of the beam line.[25] A polynomial background was subtracted from all X-ray spectra shown in this work.

Results and Discussion

Soft X-ray induced excited spin-state trapping in powder samples

First, we present the XAS measurements performed on the powder sample, which serves as a reference. Spectra recorded at 300 K and 100 K are shown in Figure 1b, above and below the SCO temperature $T_{1/2}$ = 160 K.[17] Consistent with the literature,[16,26,13] at 300 K the XAS exhibits a broad multiplet at the Fe L_3 edge with a peak at 708.2 eV characteristic of the HS state. At 100 K the Fe L_3 XAS is narrow with a peak at 709.5 eV evidencing the LS state.

SOXIESST was studied at 3 K, well below T_{LIESST} = 52 K.[17] At 3 K the HS→LS relaxation rate is negligible in the timescale of the experiments, since even at 10 K the HS state decays only by 4% in 12 h.[27] The spectrum obtained at 3 K (Figure 1b) was recorded with a small X-ray flux of $\phi = 0.04\ \mathrm{ph\ s^{-1}\ nm^{-2}}$ without prior X-ray illumination at this spot. The recording time of 120 s corresponds to a photon (ph) dose of $D = 4.8\ \mathrm{ph\ nm^{-2}}$. The HS fraction $\lambda = 1 \pm 3\%$ is obtained from the intensity ratio of the HS and LS peaks at the Fe L_3 edge. The 300 K and 100 K spectra were used as references, defining $\lambda \equiv 1$ and $\lambda \equiv 0$, respectively. This experiment shows that it is possible to study the virtually pristine LS state even in the SOXIESST regime provided that the X-ray flux is low enough. After irradiation with a significantly larger X-ray dose of

$D = 144$ ph nm^{-2}, a high-spin fraction of 77 $\pm$ 3% (Figure 1b) is observed. The SOXIESST is fully reversible, as evidenced by the recovered LS state observed at 100 K after warming up to room temperature (Figure 1b).

After these quasi-static investigations, we now follow the SOXIESST with a time resolution of 20 s by measuring the XAS intensity at distinct energies only. The high-spin fraction is calculated from the HS (E_{HS} = 708.2 eV) and LS (E_{LS} = 709.5 eV) signals normalized to the pre-edge signal. The obtained high-spin fraction $\lambda(t)$ as a function of time, recorded at 3 K using a photon flux of $\phi_0 = 0.14$ ph s^{-1} nm^{-2}, is displayed in Figure 1c. The high-spin fraction $\lambda(t)$ was fitted with the exponential function $\lambda(t) = \lambda^{\infty} - (\lambda^{\infty} - \lambda^{0})\, e^{-t/\tau}$, where $\tau = 360 \pm 15$ s is the time constant, $\lambda^{\infty} = 73 \pm 7\%$ is the HS fraction in saturation and $\lambda^{0} = 0\%$ is the initial HS fraction at t = 0. Knowing the photon flux, the time constant can be converted into a cross section $\sigma_{\mathrm{pow}} = \tau^{-1}\, \phi^{-1} = (1.96 \pm 0.08) \times 10^{-2}$ nm^2 = 196 $\pm$ 8 Mbarn, with 1 barn = 10^{-10} nm^2. We emphasize here that to the best of our knowledge this is the first quantitative report of a SOXIESST photon cross section. Interestingly, its value is ~30 times larger than the cross section of the Fe L_3 absorption edge (σ_{XAS} ~7 Mbarn).[28] This demonstrates that SOXIESST, like hard X-ray induced ESST[14] and vacuum-ultraviolet light induced ESST,[15] is not directly caused by the X-ray absorption process. SOXIESST is likely due to scattering[29–31] of the large number of secondary electrons produced after the absorption of a single X-ray photon.

Interestingly, the value of the saturation HS fraction $\lambda^{\infty} = 73 \pm 7$ % is comparable with the branching ratio at the $^3T_1$ triplet state during the initial fast relaxation after excitation into the HS or LS state, *i.e.* ~ 4 : 1 in favour of the HS state.[32] λ^{∞} also agrees well with the HS fraction of $\lambda = 77\%$ (Figure 1b) found after irradiation with an X-ray dose of $D = 144$ ph nm^{-2}.

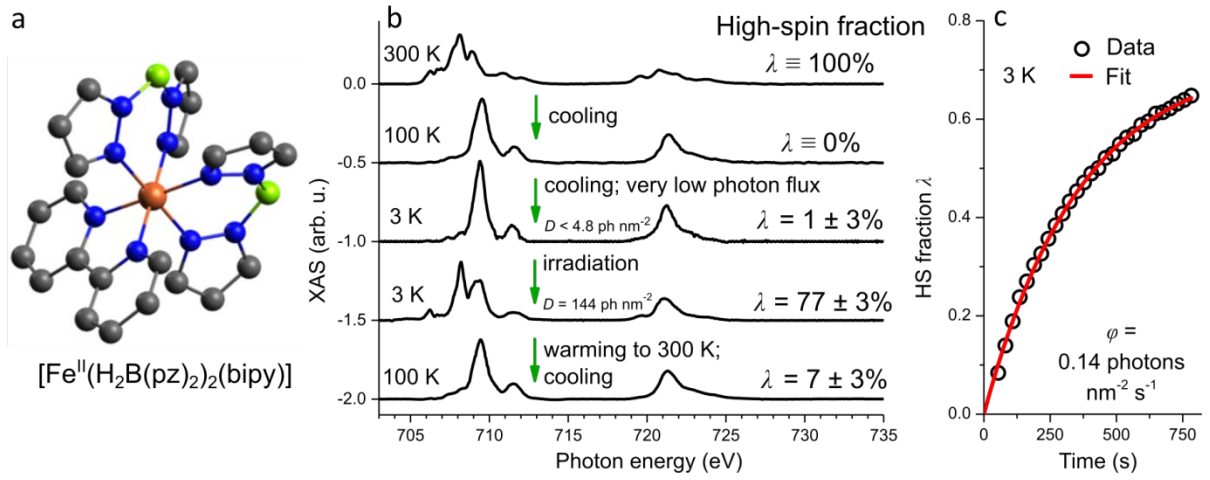

Figure 1 (a) Scheme of the SCO complex [Fe(H$_2$B(pz)$_2$)$_2$(bipy)]. Color code: orange, Fe; gray, C; blue, N; green, B. Hydrogen atoms have been omitted for clarity. (b) Sequence of X-ray spectra recorded on a powder sample of [Fe(H$_2$B(pz)$_2$)$_2$(bipy)]. The fully reversible high-spin (HS) to low-spin (LS) conversion (300 K to 100 K) and soft X-ray induced excited spin-state trapping (SOXIESST) at 3 K are visible. Spectra are offset for clarity. (c) Time-dependent HS fraction measured on the powder sample revealing the LS → HS conversion due to SOXIESST at 3 K.

It is important to distinguish the reversible SOXIESST effect from the irreversible soft X-ray photochemistry (SOXPC).[12] In order to determine the SOXPC rate, we have performed a separate experiment at 100 K where SOXIESST is not observed. The SCO powder has been irradiated with a very high photon dose $D = 550$ ph nm^{-2} (Figure 2). The spectra evidence a shoulder at lower energy corresponding to $\lambda = 0.10$. We estimate the photon cross section of SOXPC $\sigma_{\mathrm{SOXPC}} \sim 2$ Mbarn, a value which is ~100 times smaller than the cross section for the reversible SOXIESST process but nevertheless comparable to the absorption cross section of the Fe L_3 edge. The appearance of the HS signature at this temperature indicates that the molecules are irreversibly modified after the absorption of a few X-ray photons.

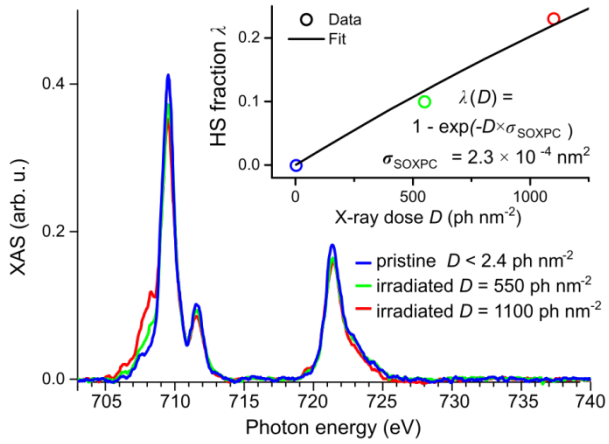

Figure 2 XAS at the Fe $L_{2,3}$ edges recorded on the powder sample after irradiation with different photon doses at 100 K. Irradiation with a very high X-ray dose results in the appearance of a shoulder at low photon energy. Assuming that only the molecules which contribute to the shoulder are irreversibly modified, we estimate the photon cross section of SOXPC σ_{SOXPC} ~ 2 Mbarn. Inset: HS fraction extracted from the XAS in the main panel as a function of the photon dose.

Soft X-ray induced spin state trapping of molecular thin films on ferroelectric substrates

The molecular thin films of ~70 nm thickness were grown on the (+) and (-) poled ferroelectric PMN-PT substrates as described in the experimental Section. Figure 3 shows the XAS of the thin films on both substrates at 300 K and 100 K, respectively. At 300 K, 94% and 93% of the molecules are found in the HS state on (-) and (+) - PMN-PT, respectively. At 100 K, the HS fraction is reduced to 33% and 24% on (-) and (+) - PMN-PT, respectively. This indicates that the thermal SCO in both thin film samples is less efficient than in the powder. The incomplete HS – LS conversion may be rationalized by a modified crystal packing, and a similar effect has been observed in other SCO thin films[18,33] as well as in SCO monolayers on graphite.[26] The origin of the slightly different HS fractions on (+) and (-) polarized PMN-PT at 100 K may be due to the adsorption of different small amounts of contaminants (*e.g.* water) on the differently polarized substrates on these *ex-situ* samples.[21,34] The difference may also be related to the

observations reported in ref. 24 where a complete suppression of the thermal (HS → LS) SCO down to 100 K was reported for one of the two polarizations of an organic ferroelectric thin film. However, we note that the total magnetic moment reported in ref. 24 appears too large compared to the reported film thickness.

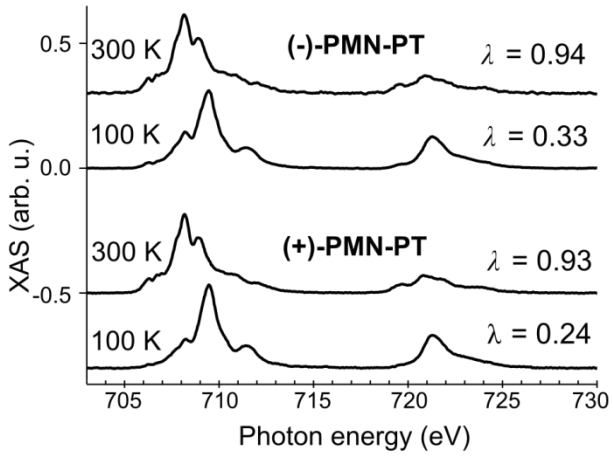

Figure 3 Temperature dependent XAS recorded on ~70 nm thick molecular films on (+) and (-) polarized ferroelectric PMN-PT substrates. The molecules are predominantly in the HS state at 300 K and in the LS state at 100 K. The spectra have been offset for clarity.

Next we discuss SOXIESST in the thin film samples at 3 K, *i.e.* below T_{LIESST} where also SOXIESST can occur. Figure 4a and 4b display two sequences of six XAS spectra each on (-) and (+)-PMN-PT, respectively. At the used photon flux $\phi_0 = 0.14$ ph s^{-1} nm^{-2}, each spectrum has an acquisition time $t = 144$ s resulting in a dose of 20 ph nm^{-2}. Remarkably, we observe virtually no SOXIESST on the (-) poled substrate, while on the (+) poled sample a significant HS fraction appears within minutes of irradiation. This is also seen in the extracted HS fractions (Figure 4c).

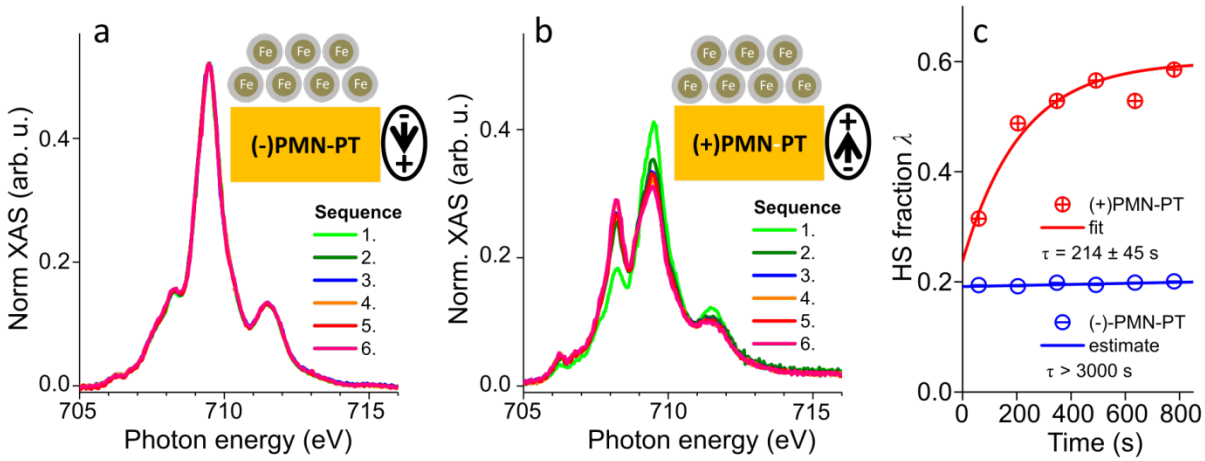

Figure 4 XAS of the thin films at 3 K on (+) and (-) polarized ferroelectric PMN-PT. (a,b) Sequence of 6 spectra on both substrates showing the Fe L_3 edge, respectively. $\phi_0 = 0.14$ ph s^{-1} nm^{-2}, each spectrum corresponds to a X-ray dose of $D = 20$ ph nm^{-2}. Spin-state trapping is observed on (+)-PMN-PT but not on (-)-PMN-PT. The spectra have been normalized to the same Fe L_3 peak area for visibility. (c) Time dependent HS fractions extracted from the spectra shown in (a,b).

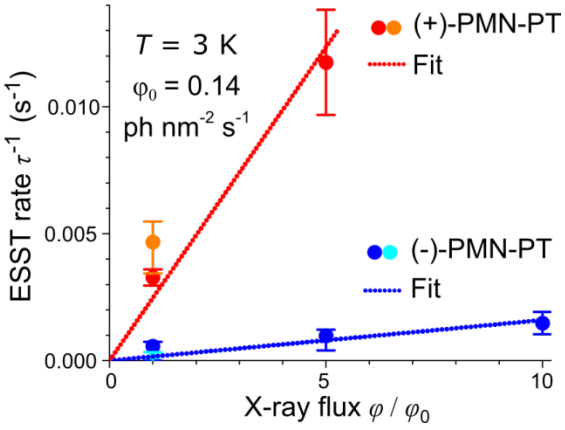

Figure 5 Comparison of flux dependent ESST rates $\tau^{-1}(\phi)$. Dashed lines denote linear fits $\sigma = \tau^{-1}\,\phi^{-1}$ to the data. The resulting ESST cross sections σ are reported in Table 1. The orange and light blue data points correspond to the rate constants obtained from sequences of spectra (Figure 4). The red and blue data points have been obtained by measuring XAS at discrete energies.

The SOXIESST rates $\tau^{-1}(\phi)$ recorded as a function of the X-ray flux ϕ are shown in Figure 5. The figure combines the rates obtained from the spectra with measurements at discrete energies. Both methods yield consistent values within the error. The data confirm that the rates for SOXIESST on the differently polarized substrates are both proportional to the X-ray flux. The corresponding values for the ESST cross sections $\sigma = \tau^{-1}\,\phi^{-1}$ on the different samples are listed in Table 1. We emphasize that the cross section $\sigma_{(+)}$ is similar to the one in the powder, while the cross section $\sigma_{(-)}$ is more than one order of magnitude lower. This is in accordance with the different time evolution of the XAS shown in Figure 4. The striking difference between the SOXIESST cross sections is another strong evidence that the SOXIESST mechanism is more complicated than simply the absorption of a X-ray photon and subsequent de-excitation of the Fe(II) ion.

Table 1 Excited spin-state trapping cross sections σ at 3 K for $[Fe(H_2B(pz)_2)_2(bipy)]$ SCO complexes in powder form as well as for thin films on the ferroelectric substrates.

Sample	**σ (Mbarn)**
SCO powder	196 ± 8
SCO on (+)-PMN-PT	174 ± 22
SCO on (-)-PMN-PT	12 ± 2

In order to shed light on the surprising difference in the ESST cross sections of the SCO thin films on the (+) and (-) polarized PMN-PT, we have analyzed the sequences of X-ray spectra obtained at 300 K and 3 K (Figures 4a,b) each of which have been taken on fresh spots on the surface. X-ray illumination commenced at $t = 0$. Figure 6a displays the time dependent intensity

of the pre-edge TEY signals obtained at a photon energy of 704 eV from the X-ray spectra. A signal of 1 arb. u. in Figure 6a on the ordinate corresponds to ~0.4 nA of TEY current from the sample. Compared to 300 K, the TEY is significantly reduced at 3 K on both samples and a strong decay in time is observed. Remarkably, at low temperature there is a sizeable difference between the signals from the (+) and (-)-poled substrates which will be discussed further below. The integral of the Fe $L_{2;3}$ peaks divided by the pre-edge signal is shown in Figure 6b. An increase over time is observed at low temperature, which is more pronounced for the (+)-poled substrate.

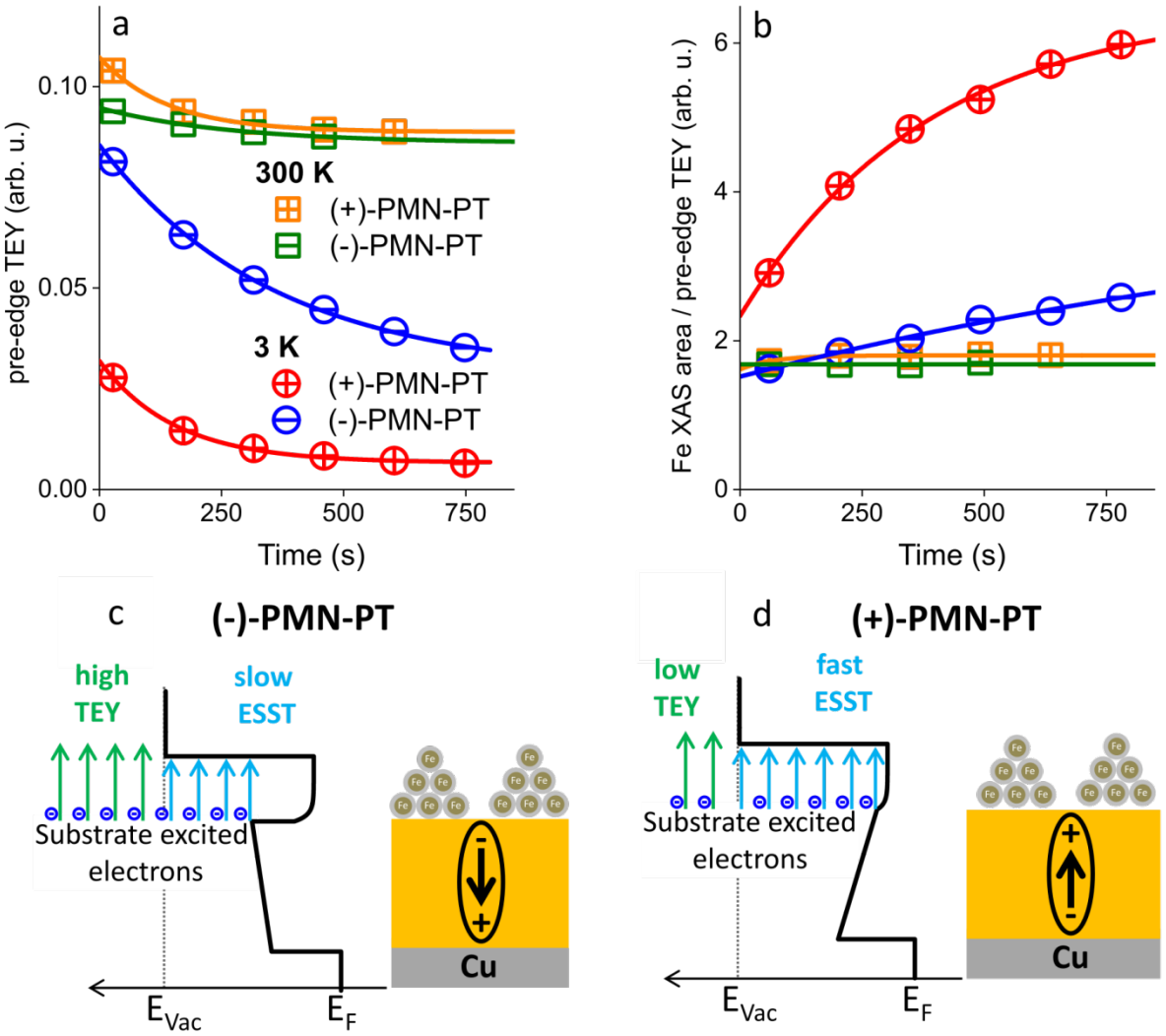

Figure 6 Data extracted from sequences of X-ray spectra of the SCO thin films on (+) and (-)-PMN-PT at 300 K and 3 K. (a) Time dependent pre-edge TEY obtained at a photon energy of 704 eV. (b) Time dependent integrated area of the Fe $L_{2;3}$ peaks normalized by the pre-edge TEY shown in panel (a). (c,d) Sketches of the lower conduction band edge of the (+) and (-) polarized PMN-PT substrates at low temperature, neglecting interface dipole effects. Green (blue) arrows denote X-ray excited substrate electrons with sufficient (insufficient) kinetic energy to leave the sample. A larger rate of electrons remaining in the sample results in a higher SOXIESST rate.

The data shown in Figures 6a,b reveal a different behavior of the Fe XAS and the one of the pre-edge. While the Fe signal originates from the molecules, the pre-edge signal has contributions from the molecular ligand as well as from the substrate. The contribution of the latter depends on the exact sample morphology since the XAS probing depth is given by the electron escape depth of a few nm. Since the molecular ligand is unlikely to show charging different from the Fe(II) center ion we deduce that the pre-edge TEY contains a significant amount of substrate electrons which can be easily understood by the presence of empty surface areas related to the frequently observed inhomogeneous molecular island (Volmer-Weber) growth.

We attribute the time dependent decrease of the pre-edge signal (Figure 6a) to charge depletion which is commonly observed on insulating substrates under X-ray irradiation[35] because of the removal of electrons from the surface. The charging leads to an increase of the electron affinity and thus reduces the efficiency of extracting electrons from the substrate surface. The strength of the charging is given by the different, typically low, conductivities across the molecular deposit as well as through the substrate which depend on temperature and the ferroelectric polarization.[36] Note that during the X-ray measurements the TEY current density is extremely low (~100 pA mm^{-2}). The small current only allows building up small electric fields across the substrate far from the ferroelectric poling threshold.

The energy band scheme of the two samples for the low temperature case is shown in Figures 6c,d. The two different ferroelectric polarizations result in electric fields of opposite signs across the substrate, leading to different electron affinities at the surface.[34,37,38] Secondary electrons which are generated in the substrate near the surface are subjected to a larger electron affinity in the case of (+)-PMN-PT as compared to (-)-PMN-PT which results in the lower pre-edge signal observed in Figure 6a. This already happens at $t = 0$ when charging effects are not yet effective.

In the TEY mode used in this study, the signal corresponds directly to the total number of photo-, secondary- and Auger-electrons.[39,40] Only electrons with kinetic energy large enough to overcome the electron affinity leave the sample and contribute to the signal. In the case of large electron affinity there are less electrons which have sufficient energy to leave the sample, resulting in a lower TEY.[40] Therefore a larger number excited electrons remain in the sample and scatter with the molecules resulting in a faster ESST on (+)-PMN-PT. Note that in this discussion interface dipole effects have been neglected, which may lead to deviations of the band structures from the ones shown in Figures 6c,d. However, because of the low electrical conductivities of the molecules and the PMN-PT this will mainly affect the Cu/PMN-PT interface at the back, which is irrelevant for the present results and their interpretation.

The X-ray induced depletion of surface electrons discussed before leads to an increase of the electron affinity of the substrate disregarding its ferroelectric polarization. Hence it enhances the contribution of ESST-active electrons. However, we emphasize that the dependence on the ferroelectric polarization is already visible at $t = 0$ before the charging effects set in.

The cross sections for the SOXIESST effect found in our study show that the spin multiplicity (S = 0 *vs* S = 2) of the SCO complex $[Fe(H_2B(pz)_2)_2(bipy)]$ is very sensitive to X-ray radiation. The

effect works through scattering of excited electrons, as evident from the fact that its cross section is much higher than the Fe L_3 X-ray absorption cross section. In this regard, SOXIESST bears some analogy with X-ray induced demagnetization,[29–31] which affects the magnetic moments of single-molecule magnets.

Conclusions

We have performed a XAS study of SCO thin films deposited on ferroelectric PMN-PT. In the SOXIESST regime the ferroelectric polarization has a strong influence on the X-ray induced LS-to-HS conversion rate, hence the cross section for SOXIESST can be tuned by more than one order of magnitude by switching the ferroelectric polarization. The reason behind this large difference is given by the different electron affinities of the two differently poled substrates. Furthermore, we have characterized the cross sections of the SOXIESST effect as well as the one for X-ray photochemistry. The large SOXIESST cross sections indicate that one X-ray photon results in the promotion of many SCO molecules to the HS state, suggesting that the mechanism proceeds through scattering of excited secondary electrons. We anticipate that the efficiency of spin-state trapping *via* scattering with electrons can be tuned by gating the electric field. SCO complexes may also be useful as sensors for ionizing radiation and for the detection of excited electrons with energies lower than the electron affinity travelling within materials.

AUTHOR INFORMATION

Corresponding Authors

*Email: christian.waeckerlin@empa.ch, jan.dreiser@psi.ch

Notes

The authors declare no competing financial interests.

ACKNOWLEDGMENT

J.D. and C.W. gratefully acknowledge funding from the Swiss National Science Foundation (grant no. PZ00P2_142474). C.W. acknowledges financial support by the University Zurich priority program LightChEC. We thank Stephan Keller for assistance with the synthesis.

REFERENCES

(1) Létard, J.-F.; Guionneau, P.; Goux-Capes, L. Towards Spin Crossover Applications. In *Spin Crossover in Transition Metal Compounds III*; Springer-Verlag: Berlin/Heidelberg, 2004; Vol. 235, pp 221–249.

(2) Prins, F.; Monrabal-Capilla, M.; Osorio, E. A.; Coronado, E.; van der Zant, H. S. J. Room-Temperature Electrical Addressing of a Bistable Spin-Crossover Molecular System. *Adv. Mater.* **2011**, *23*, 1545–1549.

(3) Pointillart, F.; Liu, X.; Kepenekian, M.; Le Guennic, B.; Golhen, S.; Dorcet, V.; Roisnel, T.; Cador, O.; You, Z.; Hauser, J.; et al. Thermal and near-Infrared Light Induced Spin Crossover in a Mononuclear iron(II) Complex with a Tetrathiafulvalene-Fused Dipyridophenazine Ligand. *Dalton Trans* **2016**, *45*, 11267–11271.

(4) *Spin Crossover in Transition Metal Compounds*; Topics in current chemistry; Springer: Berlin ; New York, 2004.

(5) Gütlich, P. Nuclear Decay Induced Excited Spin State Trapping (NIESST). In *Spin Crossover in Transition Metal Compounds II*; Springer Berlin Heidelberg: Berlin, Heidelberg, 2004; Vol. 234, pp 231–260.

(6) Decurtins, S.; Gütlich, P.; Köhler, C. P.; Spiering, H.; Hauser, A. Light-Induced Excited Spin State Trapping in a Transition-Metal Complex: The Hexa-1-Propyltetrazole-Iron (II) Tetrafluoroborate Spin-Crossover System. *Chem. Phys. Lett.* **1984**, *105*, 1–4.

(7) Decurtins, S.; Gutlich, P.; Hasselbach, K. M.; Hauser, A.; Spiering, H. Light-Induced Excited-Spin-State Trapping in iron(II) Spin-Crossover Systems. Optical Spectroscopic and Magnetic Susceptibility Study. *Inorg. Chem.* **1985**, *24*, 2174–2178.

(8) Decurtins, S.; Gütlich, P.; Köhler, C. P.; Spiering, H. New Examples of Light-Induced Excited Spin State Trapping (LIESST) in iron(II) Spin-Crossover Systems. *J. Chem. Soc. Chem. Commun.* **1985**, 7, 430–432.

(9) Sano, H.; Gütlich, P. Hot Atom Chemistry in Relation to Mossbauer Emission Spectroscopy. In *Hot atom chemistry*; Matsuura, T., Ed.; Kodanski: Tokyo, 1984; p 265.

(10) Gopakumar, T. G.; Matino, F.; Naggert, H.; Bannwarth, A.; Tuczek, F.; Berndt, R. Electron-Induced Spin Crossover of Single Molecules in a Bilayer on Gold. *Angew. Chem. Int. Ed.* **2012**, *51*, 6262–6266.

(11) Gopakumar, T. G.; Bernien, M.; Naggert, H.; Matino, F.; Hermanns, C. F.; Bannwarth, A.; Mühlenberend, S.; Krüger, A.; Krüger, D.; Nickel, F.; et al. Spin-Crossover Complex on Au(111): Structural and Electronic Differences Between Mono- and Multilayers. *Chem. - Eur. J.* **2013**, *19*, 15702–15709.

(12) Collison, D.; Garner, C. D.; McGrath, C. M.; Mosselmans, J. F. W.; Roper, M. D.; Seddon, J. M. W.; Sinn, E.; Young, N. A. Soft X-Ray Induced Excited Spin State Trapping and Soft X-Ray Photochemistry at the Iron $L_{2,3}$ Edge in $[Fe(phen)_2(NCS)_2]$ and $[Fe(phen)_2(NCSe)_2]$ (phen = 1,10-phenanthroline). *J. Chem. Soc. Dalton Trans.* **1997**, No. 22, 4371–4376.

(13) Davesne, V.; Gruber, M.; Miyamachi, T.; Da Costa, V.; Boukari, S.; Scheurer, F.; Joly, L.; Ohresser, P.; Otero, E.; Choueikani, F.; et al. First Glimpse of the Soft X-Ray Induced Excited Spin-State Trapping Effect Dynamics on Spin Cross-over Molecules. *J. Chem. Phys.* **2013**, *139*, 074708.

(14) Vankó, G.; Renz, F.; Molnár, G.; Neisius, T.; Kárpáti, S. Hard-X-Ray-Induced Excited-Spin-State Trapping. *Angew. Chem. Int. Ed.* **2007**, *46*, 5306–5309.

(15) Ludwig, E.; Naggert, H.; Kalläne, M.; Rohlf, S.; Kröger, E.; Bannwarth, A.; Quer, A.; Rossnagel, K.; Kipp, L.; Tuczek, F. Iron(II) Spin-Crossover Complexes in Ultrathin Films: Electronic Structure and Spin-State Switching by Visible and Vacuum-UV Light. *Angew. Chem. Int. Ed.* **2014**, *53*, 3019–3023.

(16) Cartier dit Moulin, C.; Rudolf, P.; Flank, A. M.; Chen, C. T. Spin Transition Evidenced by Soft X-Ray Absorption Spectroscopy. *J. Phys. Chem.* **1992**, *96*, 6196–6198.

(17) Real, J. A.; Muñoz, M. C.; Faus, J.; Solans, X. Spin Crossover in Novel Dihydrobis(1-pyrazolyl)borate [$H_2B(pz)_2$]-Containing Iron(II) Complexes. Synthesis, X-Ray Structure, and Magnetic Properties of [$FeL\{H_2B(pz)_2\}_2$] (L = 1,10-phenanthroline and 2,2‘-bipyridine). *Inorg. Chem.* **1997**, *36*, 3008–3013.

(18) Naggert, H.; Bannwarth, A.; Chemnitz, S.; von Hofe, T.; Quandt, E.; Tuczek, F. First Observation of Light-Induced Spin Change in Vacuum Deposited Thin Films of Iron Spin Crossover Complexes. *Dalton Trans.* **2011**, *40*, 6364–6366.

(19) Yin, Z.-W.; Luo, H.-S.; Wang, P.-C.; Xu, G.-S. Growth, Characterization and Properties of Relaxor Ferroelectric PMN-PT Single Crystals. *Ferroelectrics* **1999**, *229*, 207–216.

(20) Wu, T.; Zhao, P.; Bao, M.; Bur, A.; Hockel, J. L.; Wong, K.; Mohanchandra, K. P.; Lynch, C. S.; Carman, G. P. Domain Engineered Switchable Strain States in Ferroelectric (011)

$[Pb(Mg_{1/3}Nb_{2/3})O_3]_{(1-x)}$-$[PbTiO_3]_x$(PMN-PT, x≈0.32) Single Crystals. *J. Appl. Phys.* **2011**, *109*, 124101.

(21) Zhang, Z.; González, R.; Díaz, G.; Rosa, L. G.; Ketsman, I.; Zhang, X.; Sharma, P.; Gruverman, A.; Dowben, P. A. Polarization Mediated Chemistry on Ferroelectric Polymer Surfaces. *J. Phys. Chem. C* **2011**, *115*, 13041–13046.

(22) Dowben, P. A.; Rosa, L. G.; Ilie, C. C.; Xiao, J. Adsorbate/Absorbate Interactions with Organic Ferroelectric Polymers. *J. Electron Spectrosc. Relat. Phenom.* **2009**, *174*, 10–21.

(23) Zhang, Z.; Sharma, P.; Borca, C. N.; Dowben, P. A.; Gruverman, A. Polarization-Specific Adsorption of Organic Molecules on Ferroelectric $LiNbO_3$ Surfaces. *Appl. Phys. Lett.* **2010**, *97*, 243702.

(24) Zhang, X.; Palamarciuc, T.; Létard, J.-F.; Rosa, P.; Lozada, E. V.; Torres, F.; Rosa, L. G.; Doudin, B.; Dowben, P. A. The Spin State of a Molecular Adsorbate Driven by the Ferroelectric Substrate Polarization. *Chem. Commun.* **2014**, *50*, 2255–2257.

(25) Piamonteze, C.; Flechsig, U.; Rusponi, S.; Dreiser, J.; Heidler, J.; Schmidt, M.; Wetter, R.; Calvi, M.; Schmidt, T.; Pruchova, H.; et al. X-Treme Beamline at SLS: X-Ray Magnetic Circular and Linear Dichroism at High Field and Low Temperature. *J. Synchrotron Radiat.* **2012**, *19*, 661–674.

(26) Bernien, M.; Wiedemann, D.; Hermanns, C. F.; Krüger, A.; Rolf, D.; Kroener, W.; Müller, P.; Grohmann, A.; Kuch, W. Spin Crossover in a Vacuum-Deposited Submonolayer of a Molecular Iron(II) Complex. *J. Phys. Chem. Lett.* **2012**, *3*, 3431–3434.

(27) Moliner, N.; Salmon, L.; Capes, L.; Muñoz, M. C.; Létard, J.-F.; Bousseksou, A.; Tuchagues, J.-P.; McGarvey, J. J.; Dennis, A. C.; Castro, M.; et al. Thermal and Optical

Switching of Molecular Spin States in the {[FeL[$H_2B(pz)_2]_2$} Spin-Crossover System (L = bpy, phen). *J. Phys. Chem. B* **2002**, *106*, 4276–4283.

(28) Regan, T.; Ohldag, H.; Stamm, C.; Nolting, F.; Lüning, J.; Stöhr, J.; White, R. Chemical Effects at Metal/Oxide Interfaces Studied by X-Ray-Absorption Spectroscopy. *Phys. Rev. B* **2001**, *64,* 214422.

(29) Dreiser, J.; Westerström, R.; Piamonteze, C.; Nolting, F.; Rusponi, S.; Brune, H.; Yang, S.; Popov, A.; Dunsch, L.; Greber, T. X-Ray Induced Demagnetization of Single-Molecule Magnets. *Appl. Phys. Lett.* **2014**, *105*, 032411.

(30) Wäckerlin, C.; Donati, F.; Singha, A.; Baltic, R.; Rusponi, S.; Diller, K.; Patthey, F.; Pivetta, M.; Lan, Y.; Klyatskaya, S.; et al. Giant Hysteresis of Single-Molecule Magnets Adsorbed on a Nonmagnetic Insulator. *Adv. Mater.* **2016**, *28*, 5195–5199.

(31) Donati, F.; Rusponi, S.; Stepanow, S.; Wäckerlin, C.; Singha, A.; Persichetti, L.; Baltic, R.; Diller, K.; Patthey, F.; Fernandes, E.; et al. Magnetic Remanence in Single Atoms. *Science* **2016**, *352*, 318–321.

(32) Hauser, A. Light-Induced Spin Crossover and the High-Spin→Low-Spin Relaxation. In *Spin Crossover in Transition Metal Compounds II*; Springer Berlin Heidelberg: Berlin, Heidelberg, 2004; Vol. 234, pp 155–198.

(33) Palamarciuc, T.; Oberg, J. C.; El Hallak, F.; Hirjibehedin, C. F.; Serri, M.; Heutz, S.; Létard, J.-F.; Rosa, P. Spin Crossover Materials Evaporated under Clean High Vacuum and Ultra-High Vacuum Conditions: From Thin Films to Single Molecules. *J. Mater. Chem.* **2012**, *22*, 9690–9695.

(34) Wang, J. L.; Vilquin, B.; Barrett, N. Screening of Ferroelectric Domains on BaTiO3(001) Surface by Ultraviolet Photo-Induced Charge and Dissociative Water Adsorption. *Appl. Phys. Lett.* **2012**, *101*, 092902.

(35) Vlachos, D.; Craven, A. J.; McComb, D. W. Specimen Charging in X-Ray Absorption Spectroscopy: Correction of Total Electron Yield Data from Stabilized Zirconia in the Energy Range 250–915 eV. *J. Synchrotron Radiat.* **2005**, *12*, 224–233.

(36) Choi, T.; Lee, S.; Choi, Y. J.; Kiryukhin, V.; Cheong, S.-W. Switchable Ferroelectric Diode and Photovoltaic Effect in $BiFeO_3$. *Science* **2009**, *324*, 63–66.

(37) Yang, W.-C.; Rodriguez, B. J.; Gruverman, A.; Nemanich, R. J. Polarization-Dependent Electron Affinity of $LiNbO_3$ Surfaces. *Appl. Phys. Lett.* **2004**, *85*, 2316.

(38) Barrett, N.; Rault, J. E.; Wang, J. L.; Mathieu, C.; Locatelli, A.; Mentes, T. O.; Niño, M. A.; Fusil, S.; Bibes, M.; Barthélémy, A.; et al. Full Field Electron Spectromicroscopy Applied to Ferroelectric Materials. *J. Appl. Phys.* **2013**, *113*, 187217.

(39) Stöhr, J. *NEXAFS Spectroscopy*, 1st ed. corr. print.; Springer series in surface sciences; Springer: Berlin, 1996.

(40) Henke, B.; Liesegang, J.; Smith, S. Soft-X-Ray-Induced Secondary-Electron Emission from Semiconductors and Insulators: Models and Measurements. *Phys. Rev. B* **1979**, *19*, 3004–3021.

TOC GRAPHICS

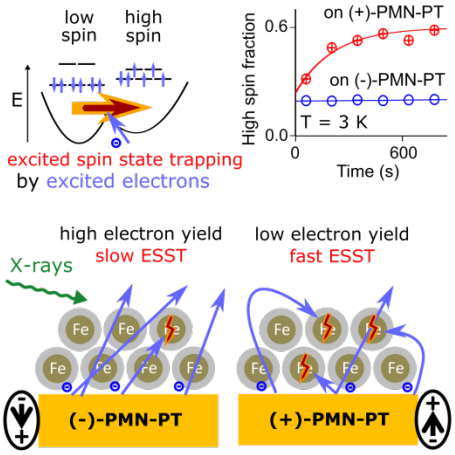
low spin
high spin
E
excited spin state trapping
by excited electrons
on (+)-PMN-PT
on (-)-PMN-PT
T = 3 K
High spin fraction
0.6
0.0
0
600
Time (s)
high electron yield
slow ESST
low electron yield
fast ESST
X-rays
Fe
(-)-PMN-PT
(+)-PMN-PT